

Inclusive jet cross section in $\bar{p}p$ collisions at $\sqrt{s} = 1.8$ TeV

F. Abe,¹⁴ H. Akimoto,³² A. Akopian,²⁷ M. G. Albrow,⁷ S. R. Amendolia,²³ D. Amidei,¹⁷ J. Antos,²⁹ C. Anway-Wiese,⁴ S. Aota,³² G. Apollinari,²⁷ T. Asakawa,³² W. Ashmanskas,¹⁵ M. Atac,⁷ P. Auchincloss,²⁶ F. Azfar,²² P. Azzi-Bacchetta,²¹ N. Bacchetta,²¹ W. Badgett,¹⁷ S. Bagdasarov,²⁷ M. W. Bailey,¹⁹ J. Bao,³⁵ P. de Barbaro,²⁶ A. Barbaro-Galtieri,¹⁵ V. E. Barnes,²⁵ B. A. Barnett,¹³ E. Barzi,⁸ G. Bauer,¹⁶ T. Baumann,⁹ F. Bedeschi,²³ S. Behrends,³ S. Belforte,²³ G. Bellettini,²³ J. Bellinger,³⁴ D. Benjamin,³¹ J. Benloch,¹⁶ J. Bensinger,³ D. Benton,²² A. Beretvas,⁷ J. P. Berge,⁷ J. Berryhill,⁵ S. Bertolucci,⁸ A. Bhatti,²⁷ K. Biery,¹² M. Binkley,⁷ D. Bisello,²¹ R. E. Blair,¹ C. Blocker,³ A. Bodek,²⁶ W. Bokhari,¹⁶ V. Bolognesi,⁷ D. Bortoletto,²⁵ J. Boudreau,²⁴ L. Breccia,² C. Bromberg,¹⁸ N. Bruner,¹⁹ E. Buckley-Geer,⁷ H. S. Budd,²⁶ K. Burkett,¹⁷ G. Busetto,²¹ A. Byon-Wagner,⁷ K. L. Byrum,¹ J. Cammerata,¹³ C. Campagnari,⁷ M. Campbell,¹⁷ A. Caner,⁷ W. Carithers,¹⁵ D. Carlsmith,³⁴ A. Castro,²¹ D. Cauz,²³ Y. Cen,²⁶ F. Cervelli,²³ H. Y. Chao,²⁹ J. Chapman,¹⁷ M.-T. Cheng,²⁹ G. Chiarelli,²³ T. Chikamatsu,³² C. N. Chiou,²⁹ L. Christofek,¹¹ S. Cihangir,⁷ A. G. Clark,²³ M. Cobal,²³ M. Contreras,⁵ J. Conway,²⁸ J. Cooper,⁷ M. Cordelli,⁸ C. Couyoumtzelis,²³ D. Crane,¹ D. Cronin-Hennessy,⁶ R. Culbertson,⁵ J. D. Cunningham,³ T. Daniels,¹⁶ F. DeJongh,⁷ S. Delchamps,⁷ S. Dell'Agnello,²³ M. Dell'Orso,²³ L. Demortier,²⁷ B. Denby,²³ M. Deninno,² P. F. Derwent,¹⁷ T. Devlin,²⁸ M. Dickson,²⁶ J. R. Dittmann,⁶ S. Donati,²³ J. Done,³⁰ T. Dorigo,²¹ A. Dunn,¹⁷ N. Eddy,¹⁷ K. Einsweiler,¹⁵ J. E. Elias,⁷ R. Ely,¹⁵ E. Engels, Jr.,²⁴ D. Errede,¹¹ S. Errede,¹¹ Q. Fan,²⁶ I. Fiori,² B. Flaughner,⁷ G. W. Foster,⁷ M. Franklin,⁹ M. Frautschi,³¹ J. Freeman,⁷ J. Friedman,¹⁶ H. Frisch,⁵ T. A. Fuess,¹ Y. Fukui,¹⁴ S. Funaki,³² G. Gagliardi,²³ S. Galeotti,²³ M. Gallinaro,²¹ M. Garcia-Sciveres,¹⁵ A. F. Garfinkel,²⁵ C. Gay,⁹ S. Geer,⁷ D. W. Gerdes,¹⁷ P. Giannetti,²³ N. Giokaris,²⁷ P. Giromini,⁸ L. Gladney,²² D. Glenzinski,¹³ M. Gold,¹⁹ J. Gonzalez,²² A. Gordon,⁹ A. T. Goshaw,⁶ K. Goulianos,²⁷ H. Grassmann,²³ L. Groer,²⁸ C. Grosso-Pilcher,⁵ G. Guillian,¹⁷ R. S. Guo,²⁹ C. Haber,¹⁵ E. Hafen,¹⁶ S. R. Hahn,⁷ R. Hamilton,⁹ R. Handler,³⁴ R. M. Hans,³⁵ K. Hara,³² A. D. Hardman,²⁵ B. Harral,²² R. M. Harris,⁷ S. A. Hauger,⁶ J. Hauser,⁴ C. Hawk,²⁸ E. Hayashi,³² J. Heinrich,²² K. D. Hoffman,²⁵ M. Hohlmann,^{1,5} C. Holck,²² R. Hollebeek,²² L. Holloway,¹¹ A. Holscher,¹² S. Hong,¹⁷ G. Houk,²² P. Hu,²⁴ B. T. Huffman,²⁴ R. Hughes,²⁶ J. Huston,¹⁸ J. Huth,⁹ J. Hylen,⁷ H. Ikeda,³² M. Incagli,²³ J. Incandela,⁷ G. Introzzi,²³ J. Iwai,³² Y. Iwata,¹⁰ H. Jensen,⁷ U. Joshi,⁷ R. W. Kadel,¹⁵ E. Kajfasz,^{7a} T. Kamon,³⁰ T. Kaneko,³² K. Karr,³³ H. Kasha,³⁵ Y. Kato,²⁰ T. A. Keaffaber,²⁵ L. Keeble,⁸ K. Kelley,¹⁶ R. D. Kennedy,²⁸ R. Kephart,⁷ P. Kesten,¹⁵ D. Kestenbaum,⁹ R. M. Keup,¹¹ H. Keutelian,⁷ F. Keyvan,⁴ B. Kharadia,¹¹ B. J. Kim,²⁶ D. H. Kim,^{7a} H. S. Kim,¹² S. B. Kim,¹⁷ S. H. Kim,³² Y. K. Kim,¹⁵ L. Kirsch,³ P. Koehn,²⁶ K. Kondo,³² J. Konigsberg,⁹ S. Kopp,⁵ K. Kordas,¹² W. Koska,⁷ E. Kovacs,^{7a} W. Kowald,⁶ M. Krasberg,¹⁷ J. Kroll,⁷ M. Kruse,²⁵ T. Kuwabara,³² E. Kuns,²⁸ A. T. Laasanen,²⁵ N. Labanca,²³ S. Lammel,⁷ J. I. Lamoureux,³ T. LeCompte,¹¹ S. Leone,²³ J. D. Lewis,⁷ P. Limon,⁷ M. Lindgren,⁴ T. M. Liss,¹¹ N. Lockyer,²²

O. Long,²² C. Loomis,²⁸ M. Loreti,²¹ J. Lu,³⁰ D. Lucchesi,²³ P. Lukens,⁷ S. Lusin,³⁴ J. Lys,¹⁵ K. Maeshima,⁷ A. Maghakian,²⁷ P. Maksimovic,¹⁶ M. Mangano,²³ J. Mansour,¹⁸ M. Mariotti,²¹ J. P. Marriner,⁷ A. Martin,¹¹ J. A. J. Matthews,¹⁹ R. Mattingly,¹⁶ P. McIntyre,³⁰ P. Melese,²⁷ A. Menzione,²³ E. Meschi,²³ S. Metzler,²² C. Miao,¹⁷ G. Michail,⁹ R. Miller,¹⁸ H. Minato,³² S. Miscetti,⁸ M. Mishina,¹⁴ H. Mitsushio,³² T. Miyamoto,³² S. Miyashita,³² Y. Morita,¹⁴ J. Mueller,²⁴ A. Mukherjee,⁷ T. Muller,⁴ P. Murat,²³ H. Nakada,³² I. Nakano,³² C. Nelson,⁷ D. Neuberger,⁴ C. Newman-Holmes,⁷ M. Ninomiya,³² L. Nodulman,¹ S. H. Oh,⁶ K. E. Ohl,³⁵ T. Ohmoto,¹⁰ T. Ohsugi,¹⁰ R. Oishi,³² M. Okabe,³² T. Okusawa,²⁰ R. Oliver,²² J. Olsen,³⁴ C. Pagliarone,² R. Paoletti,²³ V. Papadimitriou,³¹ S. P. Pappas,³⁵ S. Park,⁷ A. Parri,⁸ J. Patrick,⁷ G. Pauletta,²³ M. Paulini,¹⁵ A. Perazzo,²³ L. Pescara,²¹ M. D. Peters,¹⁵ T. J. Phillips,⁶ G. Piacentino,² M. Pillai,²⁶ K. T. Pitts,⁷ R. Plunkett,⁷ L. Pondrom,³⁴ J. Proudfoot,¹ F. Ptohos,⁹ G. Punzi,²³ K. Ragan,¹² A. Ribon,²¹ F. Rimondi,² L. Ristori,²³ W. J. Robertson,⁶ T. Rodrigo,^{7a} S. Rolli,²³ J. Romano,⁵ L. Rosenson,¹⁶ R. Roser,¹¹ W. K. Sakumoto,²⁶ D. Saltzberg,⁵ A. Sansoni,⁸ L. Santi,²³ H. Sato,³² V. Scarpine,³⁰ P. Schlabach,⁹ E. E. Schmidt,⁷ M. P. Schmidt,³⁵ A. Scribano,²³ S. Segler,⁷ S. Seidel,¹⁹ Y. Seiya,³² G. Sganos,¹² A. Sgolacchia,² M. D. Shapiro,¹⁵ N. M. Shaw,²⁵ Q. Shen,²⁵ P. F. Shepard,²⁴ M. Shimojima,³² M. Shochet,⁵ J. Siegrist,¹⁵ A. Sill,³¹ P. Sinervo,¹² P. Singh,²⁴ J. Skarha,¹³ K. Sliwa,³³ F. D. Snider,¹³ T. Song,¹⁷ J. Spalding,⁷ P. Sphicas,¹⁶ F. Spinella,²³ M. Spiropulu,⁹ L. Spiegel,⁷ L. Stanco,²¹ J. Steele,³⁴ A. Stefanini,²³ K. Strahl,¹² J. Strait,⁷ R. Ströhmer,⁹ D. Stuart,⁷ G. Sullivan,⁵ A. Soumarokov,²⁹ K. Sumorok,¹⁶ J. Suzuki,³² T. Takada,³² T. Takahashi,²⁰ T. Takano,³² K. Takikawa,³² N. Tamura,¹⁰ F. Tartarelli,²³ W. Taylor,¹² P. K. Teng,²⁹ Y. Teramoto,²⁰ S. Tether,¹⁶ D. Theriot,⁷ T. L. Thomas,¹⁹ R. Thun,¹⁷ M. Timko,³³ P. Tipton,²⁶ A. Titov,²⁷ S. Tkaczyk,⁷ D. Toback,⁵ K. Tollefson,²⁶ A. Tollestrup,⁷ J. Tonnison,²⁵ J. F. de Troconiz,⁹ S. Truitt,¹⁷ J. Tseng,¹³ N. Turini,²³ T. Uchida,³² N. Uemura,³² F. Ukegawa,²² G. Unal,²² S. C. van den Brink,²⁴ S. Vejcik, III,¹⁷ G. Velev,²³ R. Vidal,⁷ M. Vondracek,¹¹ D. Vucinic,¹⁶ R. G. Wagner,¹ R. L. Wagner,⁷ J. Wahl,⁵ C. Wang,⁶ C. H. Wang,²⁹ G. Wang,²³ J. Wang,⁵ M. J. Wang,²⁹ Q. F. Wang,²⁷ A. Warburton,¹² G. Watts,²⁶ T. Watts,²⁸ R. Webb,³⁰ C. Wei,⁶ C. Wendt,³⁴ H. Wenzel,¹⁵ W. C. Wester, III,⁷ A. B. Wicklund,¹ E. Wicklund,⁷ R. Wilkinson,²² H. H. Williams,²² P. Wilson,⁵ B. L. Winer,²⁶ D. Wolinski,¹⁷ J. Wolinski,¹⁸ X. Wu,²³ J. Wyss,²¹ A. Yagil,⁷ W. Yao,¹⁵ K. Yasuoka,³² Y. Ye,¹² G. P. Yeh,⁷ P. Yeh,²⁹ M. Yin,⁶ J. Yoh,⁷ C. Yosef,¹⁸ T. Yoshida,²⁰ D. Yovanovitch,⁷ I. Yu,³⁵ L. Yu,¹⁹ J. C. Yun,⁷ A. Zanetti,²³ F. Zetti,²³ L. Zhang,³⁴ W. Zhang,²² and S. Zucchelli²

(CDF Collaboration)

¹ Argonne National Laboratory, Argonne, Illinois 60439

² Istituto Nazionale di Fisica Nucleare, University of Bologna, I-40126 Bologna, Italy

³ Brandeis University, Waltham, Massachusetts 02254

⁴ University of California at Los Angeles, Los Angeles, California 90024

⁵ University of Chicago, Chicago, Illinois 60637

⁶ Duke University, Durham, North Carolina 27708

⁷ Fermi National Accelerator Laboratory, Batavia, Illinois 60510

- ⁸ *Laboratori Nazionali di Frascati, Istituto Nazionale di Fisica Nucleare, I-00044 Frascati, Italy*
- ⁹ *Harvard University, Cambridge, Massachusetts 02138*
- ¹⁰ *Hiroshima University, Higashi-Hiroshima 724, Japan*
- ¹¹ *University of Illinois, Urbana, Illinois 61801*
- ¹² *Institute of Particle Physics, McGill University, Montreal H3A 2T8, and University of Toronto, Toronto M5S 1A7, Canada*
- ¹³ *The Johns Hopkins University, Baltimore, Maryland 21218*
- ¹⁴ *National Laboratory for High Energy Physics (KEK), Tsukuba, Ibaraki 305, Japan*
- ¹⁵ *Lawrence Berkeley Laboratory, Berkeley, California 94720*
- ¹⁶ *Massachusetts Institute of Technology, Cambridge, Massachusetts 02139*
- ¹⁷ *University of Michigan, Ann Arbor, Michigan 48109*
- ¹⁸ *Michigan State University, East Lansing, Michigan 48824*
- ¹⁹ *University of New Mexico, Albuquerque, New Mexico 87131*
- ²⁰ *Osaka City University, Osaka 588, Japan*
- ²¹ *Universita di Padova, Istituto Nazionale di Fisica Nucleare, Sezione di Padova, I-35131 Padova, Italy*
- ²² *University of Pennsylvania, Philadelphia, Pennsylvania 19104*
- ²³ *Istituto Nazionale di Fisica Nucleare, University and Scuola Normale Superiore of Pisa, I-56100 Pisa, Italy*
- ²⁴ *University of Pittsburgh, Pittsburgh, Pennsylvania 15260*
- ²⁵ *Purdue University, West Lafayette, Indiana 47907*
- ²⁶ *University of Rochester, Rochester, New York 14627*
- ²⁷ *Rockefeller University, New York, New York 10021*
- ²⁸ *Rutgers University, Piscataway, New Jersey 08854*
- ²⁹ *Academia Sinica, Taipei, Taiwan 11529, Republic of China*
- ³⁰ *Texas A&M University, College Station, Texas 77843*
- ³¹ *Texas Tech University, Lubbock, Texas 79409*
- ³² *University of Tsukuba, Tsukuba, Ibaraki 305, Japan*
- ³³ *Tufts University, Medford, Massachusetts 02155*
- ³⁴ *University of Wisconsin, Madison, Wisconsin 53706*
- ³⁵ *Yale University, New Haven, Connecticut 06511*

Abstract

The inclusive jet differential cross section has been measured for jet transverse energies, E_T , from 15 to 440 GeV, in the pseudorapidity region $0.1 \leq |\eta| \leq 0.7$. The results are based on 19.5 pb^{-1} of data collected by the CDF collaboration at the Fermilab Tevatron collider. The data are compared with QCD predictions for various sets of parton distribution functions. The cross section for jets with $E_T > 200 \text{ GeV}$ is significantly higher than current predictions based on $\mathcal{O}(\alpha_s^3)$ perturbative QCD calculations. Various possible explanations for the high- E_T excess are discussed.

We present a precise measurement of the inclusive differential cross section for jet production in $p\bar{p}$ collisions at 1.8 TeV. Our measurement is compared to next-to-leading order (NLO) perturbative QCD predictions [1] for jet transverse energies, E_T , from 15 to 440 GeV in the central pseudorapidity region $0.1 \leq |\eta| \leq 0.7$, corresponding at highest E_T to a distance scale of $O(10^{-17})$ cm.

The predictions depend on details of the parton distribution functions (PDFs) and on the strong coupling constant α_S . Our measurement provides precise information about both [2, 3]. Apart from these theoretical uncertainties, deviations of the predicted cross section from experiment could arise from physics beyond the Standard Model. In particular, the presence of quark substructure would enhance the cross section at high E_T . Previous measurements of inclusive jet production were performed with smaller data sets by CDF [4, 5] and at lower energy by UA2 [6] and CDF [7].

The measurement described here is based on a data sample of 19.5 pb^{-1} collected in 1992-93 with the CDF detector[8] at the Tevatron collider. The data were collected using several triggers with jet E_T thresholds of 100, 70, 50 and 20 GeV. The 70, 50 and 20 GeV triggers were prescaled by 6, 20 and 500, respectively. Cosmic rays and accelerator loss backgrounds were removed with cuts on event energy timing and on missing transverse energy, as described in reference [5]. The remaining backgrounds are conservatively estimated to be $<0.5\%$ in any E_T bin.

Jets were reconstructed using a cone algorithm[9] with radius $R \equiv (\Delta\eta^2 + \Delta\phi^2)^{1/2} = 0.7$. Here $\eta \equiv -\ln[\tan(\theta/2)]$, where θ is the polar angle with respect to the beam line and ϕ is the azimuthal angle around the beam. The QCD calculation used a similar algorithm[1]. The ambient energy from fragmentation of partons not associated with the hard scattering is subtracted. No correction is applied for the energy falling outside the cone because this effect is modelled by the NLO QCD calculations.

The measured jet E_T spectrum is corrected for detector and smearing effects caused by finite E_T resolution with the “unsmearing procedure” described in [7]. A Monte Carlo simulation, based on the ISAJET[10] program and Feynman-Field[11] jet fragmentation tuned to the CDF data, is used to determine detector response functions. A trial true (unsmearred) spectrum is smeared with detector effects and compared to the raw data. The parameters of the trial spectrum are iterated to obtain the best match between the smeared trial spectrum and the raw data. We parameterize the unsmearred inclusive jet spectrum with the functional form

$$\frac{d\sigma(E_T^{True})}{dE_T^{True}} = P_0 \times (1 - x_T)^{P_6} \times 10^{F(E_T^{True})}, \quad (1)$$

where $F(x) = \sum_{i=1}^5 P_i \times [\log(x)]^i$ with E_T^{True} in GeV, $P_0 \dots P_6$ are fitted parameters and x_T is defined as $2E_T^{True}/\sqrt{s}$. The resulting fit of the smeared true spectrum to our data yields $\chi^2/\text{degree-of-freedom} \equiv \chi^2/d.f. = 29.9/34$. The best-fit set of parameters for Eq. 1, i.e. the “standard curve”, are in Table 1. Corrections to the measured E_T and rate for each bin of the raw spectrum are derived from the mapping of the standard curve to the smeared curve. The corrected cross sections and statistical uncertainties are in Fig. 1 and in Table 2.

To evaluate systematic uncertainties, the procedure in reference [7] is used. New parameter sets for Eq. 1 are derived for ± 1 standard deviation shifts in the unsmearing function for each source of systematic uncertainty. The parameters for the eight largest systematic uncertainties are in Table 1. They account for the following uncertainties: (a) charged hadron response at high P_T ; (b) the calorimeter response to low- P_T hadrons; (c) $\pm 1\%$ on the jet energy for the absolute calibration of the calorimeter; (d) jet fragmentation functions used in the simulation; (e) $\pm 30\%$ on the underlying event energy in a jet cone; (f) detector response to electrons and photons and (g) modeling of the detector jet energy resolution. An overall normalization uncertainty of $\pm 3.8\%$ was derived from the uncertainty in the luminosity measurement ($\pm 3.5\%$) and the efficiency of the acceptance cuts ($\pm 1.5\%$). Additional tests of the unsmearing procedure, including use of the HERWIG Monte Carlo program[13] to model jet fragmentation, were performed and the resulting variations were found to be small. Fig. 2(a–h) shows the percentage change from the standard curve as a function of E_T for each uncertainty.

In Fig. 1 the corrected cross section is compared with the NLO QCD prediction [1] using MRSD0' PDFs[12], with renormalization/factorization scale $\mu = E_T/2$. These results show excellent agreement in shape and in normalization for $E_T < 200$ GeV, while the cross section falls by six orders of magnitude. Above 200 GeV, the CDF cross section is significantly higher than the NLO QCD prediction. These data are consistent with our previous measurement [4], which also shows an excess over NLO QCD for the $E_T > 280$ GeV region. A similar excess is observed when we compare CDF data with HERWIG Monte Carlo predictions.

The distributions of the physical variables in the 1192 events above 200 GeV were examined carefully. Data distributions sensitive to the mismeasurement of jet E_T , such as unbalanced jet E_T in dijet events, show good agreement with detector simulation. To look for time and luminosity dependent variations (instantaneous luminosity increased with time), the data were divided into seven time-ordered parts and analyzed independently. No significant time dependence was observed. Finally, these events were individually scanned and no anomalies were discovered.

No single experimental source of systematic uncertainty can account for the high- E_T excess. For example, in order to reconcile the measured CDF spectrum with NLO QCD (MRSD0', $\mu = E_T/2$) predictions, we would have to change the jet E_T scale by an amount ranging from 0.2% at 175 GeV to 5% at 415 GeV, while keeping the change less than 0.1% between 50 and 160 GeV. No known feature of the detector, its calibration or the data analysis permits such a change. The effects of all possible combinations of the systematic uncertainties are included in the comparison described below.

To analyze the significance of this excess we use four statistical tests: signed and unsigned Kolmogorov-Smirnov [14], Smirnov-Cramèr-VonMises [14], and Anderson-Darling [15, 16]. For this comparison we choose the MRSD0' PDFs which provide the best description of our low E_T data. The eight sources of systematic uncertainty are treated individually to include the E_T dependence of each uncertainty. The effect of finite binning and systematic uncertainties are modelled by a Monte Carlo calculation. The statistical tests over the full E_T range are dominated by the higher precision data at low E_T ; therefore, we test two ranges. Between 40 and 150 GeV, the agreement between data

and theory is $>80\%$ for all four tests. Above 150 GeV, however, each of the four methods yields a probability of 1% that the excess is due to a fluctuation.

We have considered various sources of uncertainty in the theory. The NLO QCD predictions have a weak dependence on the renormalization/factorization scale μ . The change in μ scale from $2 E_T$ to $E_T/4$ changes the normalization but maintains the shape for $E_T > 70$ GeV [17]. For the NLO QCD calculations the renormalization and factorization scales have been assumed to be equal. Varying these scales independently also has little effect on the shape of the theoretical curve[18]. However, soft gluon summation may lead to a small increase in the cross section at high E_T [19, 20]. In addition, the effect of higher order QCD corrections is not known.

The fractional difference between the MRSD0' [12] NLO QCD predictions and predictions using different choices of published PDFs, with $\mu = E_T/2$, is shown in Fig.1. The excess of data over theory at high E_T remains for CTEQ2M[21], CTEQ2ML[21], GRV94[22], MRSA'[23] and MRSG[24] parton distributions. The variations in QCD predictions represent a survey of currently available distributions. They do not represent uncertainties associated with data used in deriving the PDFs. Inclusion of our data in a global fit with those from other experiments may yield a consistent set of PDFs that accommodate the high- E_T excess within the scope of QCD [3, 25].

The presence of quark substructure could appear as an enhancement of the cross section at high E_T . This effect is conventionally parameterized in terms of a contact term of unit strength between left-handed quarks, characterized by the constant Λ_C with units of energy [26]. While NLO standard model QCD predictions have been available for many years, no calculation for compositeness at next-to-leading order [$O(\alpha_s^3)$] is available. Therefore, we have compared our data to a LO QCD calculation including compositeness (using MRSD0') and have taken the approach of reference [4]. We normalize the predicted cross section to the data over the E_T range 95-145 GeV, where the effect of the contact term with $\Lambda_C > 1000$ GeV is small. The best agreement between this calculation and our data above $E_T > 200$ GeV is for $\Lambda_C = 1600$ GeV. This hypothetical contact interaction is also expected to lead to dijet production with a more central angular distribution, and this analysis is underway. However, until a realistic method for representing the theoretical uncertainties from higher order QCD corrections and from the PDFs is found, any claim about the presence or absence of new physics is not defensible.

In summary, we have measured the inclusive jet cross section in the E_T range 15-440 GeV and find it to be in good agreement with NLO QCD predictions for $E_T < 200$ GeV using MRSD0' PDFs. Above 200 GeV, the jet cross section is significantly higher than the NLO predictions. The data over the full E_T range are very precise. They provide powerful constraints on QCD, and demand a reevaluation of theoretical predictions and uncertainties within and beyond the Standard Model.

We thank the Fermilab staff and the technical staffs of the participating institutions for their vital contributions. This work was supported by the U.S. Department of Energy and National Science Foundation; the Italian Istituto Nazionale di Fisica Nucleare; the Ministry of Education, Science and Culture of Japan; the Natural Sciences and Engineering Research Council of Canada; the National Science Council of the Republic of China;

and the A. P. Sloan Foundation.

References

- [1] S. Ellis, Z. Kunszt, and D. Soper, Phys. Rev. Lett. **62** 2188 (1989), Phys. Rev. Lett. **64** 2121 (1990).
- [2] W. T. Giele, E.W.N. Glover and J. Yu, FERMILAB-PUB-127-T, DTP/95/52. hep-ph/9506442 (1995).
- [3] J. Huston *et al.*, MSU-HEP-50812, FSU-HEP-951031, CTEQ-512 (1995).
- [4] CDF Collaboration, F. Abe *et al.*, Phys. Rev. Lett. **68** 1104 (1992).
- [5] CDF Collaboration, F. Abe *et al.*, Phys. Rev. Lett. **62** 613 (1989).
- [6] UA2 Collaboration, J. Alitti *et al.*, Phys. Lett. **B257**, 232(1991).
- [7] CDF Collaboration, F. Abe *et al.*, Phys. Rev. Lett. **70** 1376 (1993).
- [8] CDF Collaboration, F. Abe *et al.*, Nucl. Instrum. Methods **A271**, 387 (1988).
- [9] CDF Collaboration, F. Abe *et al.*, Phys. Rev. D **45** 1448 (1992).
- [10] F.Paige and S.Protopopescu, Brookhaven Nat. Lab. Report No. BNL-38034 (1986) (unpublished).
- [11] R.Field and R.Feynman, Nucl. Phys. **B136** 1 (1978).
- [12] A.D. Martin, R.G. Roberts and W.J. Stirling, Phys.Lett. **B306** 145 (1993).
- [13] G. Marchesini and B. R. Webber, Nucl. Phys. **B310**, 461 (1988).
- [14] See, for example, “Probability and Statistics in Experimental Physics”, by Byron Roe, Springer-Verlag, New York, (1992).
- [15] T.W. Anderson and D.A.Darling, Ann.Math.Stat **23**,193-212 (1952).
- [16] T.W. Anderson and D.A.Darling, J.Amer.Stat.Assoc. **49**,765-769 (1954).
- [17] A. Bhatti, for the CDF Collaboration, presented at *The 10th Topical Workshop on Proton-Antiproton Collider Physics*, Batavia, Illinois, May 1995; Fermilab-Conf-95-192-E.
- [18] D. Soper, private communication.
- [19] Walter Giele, presented at *The 10th Topical Workshop on Proton-Antiproton Collider Physics*, Batavia, Illinois, May 1995; Fermilab-Conf-95-169-T.

Table 1: Parameters of the curves corresponding to ± 1 -standard deviation changes in the systematic uncertainties.

	P_0 (nb/GeV)	P_1	P_2	P_3	P_4	P_5	P_6
Standard	3.090×10^8	-4.128	1.084	-0.845	0.136	0.00279	6.733
High P_T pion(+)	3.000×10^8	-4.110	1.083	-0.847	0.135	0.00213	6.500
High P_T pion(-)	3.118×10^8	-4.132	1.084	-0.844	0.137	0.00299	6.758
Low P_T pion (+)	3.135×10^8	-4.163	1.082	-0.843	0.138	0.00342	7.209
Low P_T pion (-)	3.060×10^8	-4.096	1.085	-0.847	0.135	0.00216	6.272
1.0% E. scale(+)	3.174×10^8	-4.122	1.083	-0.846	0.136	0.00270	6.434
1.0% E. scale(-)	3.066×10^8	-4.140	1.084	-0.844	0.137	0.00274	7.082
Fragmentation (+)	3.152×10^8	-4.161	1.082	-0.843	0.138	0.00335	7.214
Fragmentation (-)	3.044×10^8	-4.095	1.085	-0.847	0.135	0.00220	6.229
Underly. Energy(+)	6.630×10^8	-4.314	1.067	-0.840	0.141	0.00503	8.045
Underly. Energy(-)	1.730×10^8	-4.004	1.099	-0.846	0.134	0.00122	6.074
Electron/ γ (+)	3.102×10^8	-4.123	1.084	-0.845	0.136	0.00271	6.629
Electron/ γ (-)	3.106×10^8	-4.138	1.083	-0.844	0.137	0.00287	6.873
Resolution (+)	2.422×10^8	-4.082	1.090	-0.845	0.136	0.00222	6.645
Resolution (-)	4.262×10^8	-4.201	1.076	-0.843	0.138	0.00366	7.123

- [20] G. Sterman, presented at *The 10th Topical Workshop on Proton-Antiproton Collider Physics*, Batavia, Illinois, May 1995; ITP-SB-95-30, hep-ph/950835.
- [21] James Bott *et al.*, Phys. Lett. **B304** 159 (1993).
- [22] M. Gluck, E. Reya and R. Vogt, Z. Phys. **C67** 433 (1995).
- [23] A.D. Martin, R.G. Roberts and W.J. Stirling, Phys. Rev. **D50** 6734 (1994).
- [24] A.D. Martin, R.G. Roberts and W.J. Stirling Phys. Lett. **B354** 155 (1995).
- [25] A.D. Martin, R.G. Roberts, K.J. Stevenson and W.J. Stirling, private communication.
- [26] E. Eichten, K. Lane, and M. Peskin, Phys. Rev. Lett. **50**, 811 (1983).

Table 2: The mean true jet E_T , cross section and statistical uncertainty.

$\langle E_T \rangle$ (GeV)	Cross Section (nb/GeV)	$\langle E_T \rangle$ (GeV)	Cross Section (nb/GeV)
14.5	$(1.14 \pm 0.03) \times 10^4$	133.8	$(8.50 \pm 0.12) \times 10^{-2}$
20.3	$(2.31 \pm 0.12) \times 10^3$	139.2	$(6.62 \pm 0.10) \times 10^{-2}$
26.9	$(6.30 \pm 0.56) \times 10^2$	144.5	$(5.00 \pm 0.08) \times 10^{-2}$
33.3	$(2.36 \pm 0.09) \times 10^2$	149.9	$(3.92 \pm 0.07) \times 10^{-2}$
39.5	$(1.02 \pm 0.01) \times 10^2$	155.3	$(3.13 \pm 0.06) \times 10^{-2}$
45.5	$(4.89 \pm 0.06) \times 10^1$	160.7	$(2.46 \pm 0.05) \times 10^{-2}$
51.3	$(2.61 \pm 0.04) \times 10^1$	168.4	$(1.75 \pm 0.03) \times 10^{-2}$
57.0	$(1.42 \pm 0.03) \times 10^1$	179.2	$(1.10 \pm 0.02) \times 10^{-2}$
62.7	$(8.62 \pm 0.21) \times 10^0$	189.0	$(7.34 \pm 0.20) \times 10^{-3}$
68.3	$(5.43 \pm 0.16) \times 10^0$	200.7	$(5.11 \pm 0.17) \times 10^{-3}$
73.9	$(3.24 \pm 0.13) \times 10^0$	211.5	$(3.41 \pm 0.13) \times 10^{-3}$
79.4	$(2.05 \pm 0.10) \times 10^0$	224.6	$(2.25 \pm 0.09) \times 10^{-3}$
85.0	$(1.44 \pm 0.02) \times 10^0$	240.9	$(1.14 \pm 0.06) \times 10^{-3}$
90.5	$(1.02 \pm 0.02) \times 10^0$	257.2	$(6.67 \pm 0.47) \times 10^{-4}$
95.9	$(6.94 \pm 0.13) \times 10^{-1}$	273.5	$(4.31 \pm 0.38) \times 10^{-4}$
101.4	$(5.18 \pm 0.11) \times 10^{-1}$	292.0	$(2.50 \pm 0.25) \times 10^{-4}$
106.8	$(3.64 \pm 0.05) \times 10^{-1}$	313.7	$(1.35 \pm 0.19) \times 10^{-4}$
112.2	$(2.64 \pm 0.04) \times 10^{-1}$	335.3	$(6.37 \pm 1.30) \times 10^{-5}$
117.6	$(2.00 \pm 0.04) \times 10^{-1}$	364.0	$(3.03 \pm 0.66) \times 10^{-5}$
123.0	$(1.48 \pm 0.03) \times 10^{-1}$	414.9	$(9.05 \pm 2.86) \times 10^{-6}$
128.4	$(1.10 \pm 0.03) \times 10^{-1}$		

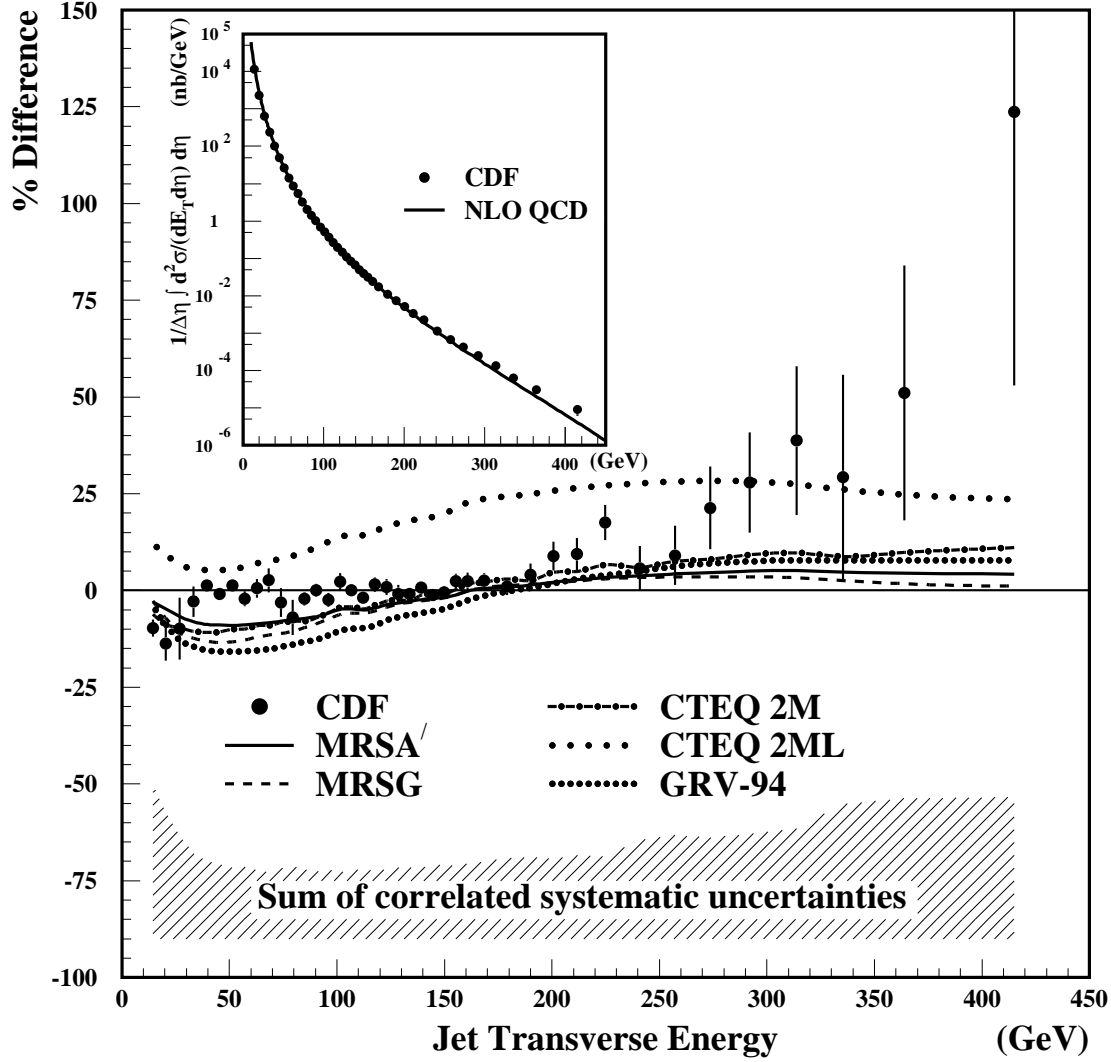


Figure 1: The percent difference between the CDF inclusive jet cross section (points) and a next-to-leading order (NLO) QCD prediction using MRSD0' PDFs. The CDF data (points) are compared directly to the NLO QCD prediction (line) in the inset. The normalization shown is absolute. The hatched region at the bottom shows the quadratic sum of correlated systematic uncertainties. NLO QCD predictions using different PDFs are also compared with the one using MRSD0'.

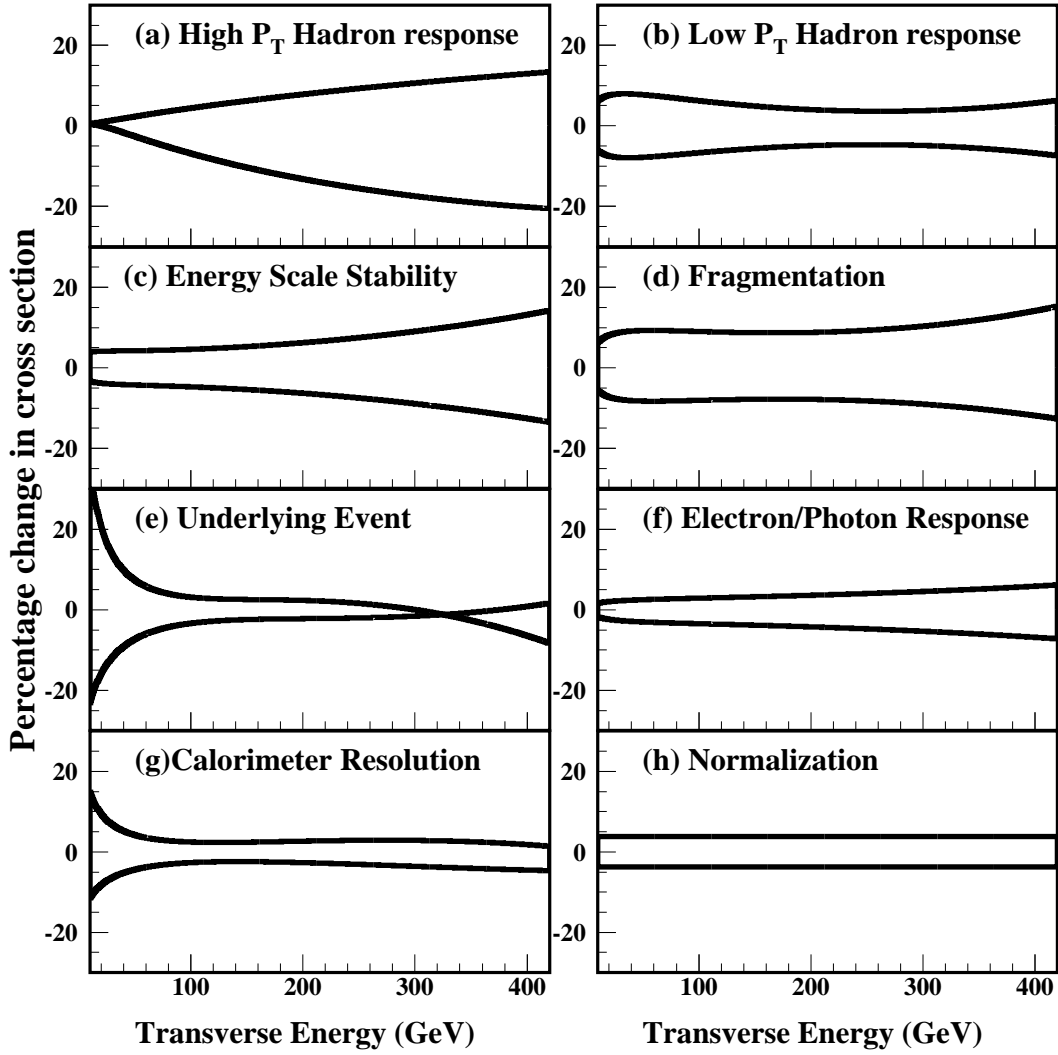


Figure 2: The percentage change in the inclusive jet cross section when various sources of systematic uncertainty are changed by ± 1 -standard deviation from their nominal values.